

Geometric based apple suction strategy for robotic packaging

Zhong Wang^{1†}, Qingyu Wang^{2,3†}, Mingzhao Lou^{2,3}, Fan Wu^{2,3}, Yaonan Zhu⁴,
Dong Hu¹, Mingchuan Zhou^{2,3}, Yibin Ying^{2,3*}

(1. College of Optical, Mechanical and Electrical Engineering, Zhejiang A&F University, Hangzhou 311300, China;

2. College of Biosystems Engineering and Food Science, Zhejiang University, Hangzhou 310058, China;

3. Key Laboratory of Intelligent Equipment and Robotics for Agriculture of Zhejiang Province, Zhejiang University, Hangzhou 310058, China;

4. Department of Micro-Nona Mechanical Science and Engineering, Nagoya University, Furo-cho, Chikusa-ku, Nagoya 464-8601, Japan)

Abstract: Packaging is one of the least automated steps among all the fruit postharvest processes, which is time-consuming and labor-intensive. Therefore, a robust suction strategy for robotic manipulation needs to be developed. In this research, a geometric-based apple suction strategy for robotic packaging was studied, including suction cup design, optimal suction region selection algorithm, and robot system integration. In the first place, on the basis of the geometric features of the spheroid fruit, the structure of the suction cups was designed to provide reliable suction force. Then, suction force measurement experiments on both acrylic balls and apples were conducted. Based on the results, the parameters of the suction cup were finally determined. The results also indicated that the curvature radius of the suction region is supposed to larger than that of the suction cups. Furthermore, a robust suction region selection algorithm was developed, which involves four steps: RGB-D information acquisition, object detection and point cloud generation, spherical fitting, and suction region selection. Finally, the above methods were integrated into a robotic packaging system. In addition, on the basis of spatial-frequency domain imaging (SFDI) technology, early stage bruise was detected for validation. The results showed that, the proposed suction strategy and system is potential for robust robotic apple packaging.

Keywords: apple, suction cup, robotic packaging, robotic manipulation, point cloud

DOI: [10.25165/ijabe.20241703.7947](https://doi.org/10.25165/ijabe.20241703.7947)

Citation: Wang Z, Wang Q Y, Lou M Z, Wu F, Zhu Y N, Hu D, et al. Geometric based apple suction strategy for robotic packaging. *Int J Agric & Biol Eng*, 2024; 17(3): 12–20.

1 Introduction

By the end of 2020, the annual yield of fruit maintains sustained growth and reached 8.87×10^8 t. Nearly all kinds of and all of the fruit need to go through the commercialization processes, including uploading, safety and quality detection^[1], grading^[2], and packaging. Among all these steps, packaging is an important step that can extend product shelf life, realize the added value of products, and achieve information traceability^[3]. However, packaging is currently the least automated step, which is time-consuming and labor-intensive. This to some extent, limits the deployment of the fruit sorting industry. In recent years, robotics has shown great potential in shelf manipulation, such as pick, carry,

and place. Therefore, it is supposed to use robots to achieve automated fruit packaging and solve the problem of an aging population^[4-7].

In general, grasping and suction are two typical robot manipulation methods^[8,9]. Both methods have been widely used in warehouses or factories to achieve monotonous tasks, such as stacking, pick-and-place. As for grasping, parallel-jaw and multi-finger grippers are two major end effectors employed to grasp objects by force- or form-closure approaches. Suction method generally picking an object by using the pressure difference^[10,11]. Meanwhile, both grasping and suction have their advantages and disadvantages. Grasping can achieve more dexterous manipulation depending on more degree of freedom^[12]. It is appropriate to pick up objects with wrinkled or discontinuous surfaces. However, it is sensitive to complex sizes and shapes of the objects and can leads to higher failure rates compared with suction manipulation^[6,13]. Suction has the advantage of being robust, less likely to cause damage, and less limited in terms of the shapes and sizes of the objects^[14,15]. As is known to all, fresh fruit is fragile and heterogeneous product, which makes it a perpetual challenge for the application of robots. Thus, suction is more suitable for fresh fruit manipulation, which usually has continuous and smooth surfaces, such as apples, pears, and peaches.

The design of the suction cup and the development of a suction region selection algorithm appropriate for fruit are two core challenges, which directly influence the efficiency and success rate. In recent years, researchers have done a lot of research about these two problems, while there are many issues that remain to be unsolved.

Automatic packaging based on suction has been commonly

Received date: 2022-10-02 **Accepted date:** 2023-07-02

Biographies: Zhong Wang, MS, research interest: machine vision, agricultural robot, Email: wangz@stu.zafu.edu.cn; Qingyu Wang, PhD candidate, research interest: agricultural robot, robotic vision and tactile robotics, Email: 12013027@zju.edu.cn; Mingzhao Lou, PhD candidate, research interest: 3D reconstruction and agricultural robot, Email: 11913014@zju.edu.cn; Fan Wu, UG, research interest: agricultural robot, data analysis, Email: fan.wu@zju.edu.cn; Yaonan Zhu, PhD, Assistant Professor, research interest: tele-robotics and force control, haptic feedback and dexterous manipulators, Email: zhu@robo.mein.nagoya-u.ac.jp; Dong Hu, PhD, Associate Professor, research interest: sensing technology for agro-product, Email: 20180047@zafu.edu.cn; Mingchuan Zhou, PhD, Assistant Professor, research interest: agricultural robot and machine vision, Email: mczhou@zju.edu.cn.

†These authors contributed equally to this work.

*Corresponding author: Yibin Ying, PhD, Qiushi Distinguished Professor, Fellow, ASABE, research interest: agricultural robot and sensing technology for agro-products. College of Biosystems Engineering and Food Science, Zhejiang University, No.866 Yuhangtang Road, Hangzhou 310058, China. Tel: +86-571-88982885, Email: ibeying@zju.edu.cn.

used in many countries. Lots of commercial suction cups have appeared in the market. However, suction cups are usually selected empirically without scientific guidance. Thus, it is difficult to guarantee stable contact between suction cups and fruit. Besides, being inspired by bionics, researchers also applied many kinds of new materials^[16-19] to manufacture innovative suction cups and even append force sensing capability^[7,20] to the soft suction cups. Nevertheless, lots of research findings are still in the experimental stage and are not appropriate for commercial usage. Above all, it is essential to explore the suction mechanism between the suction cup and spheroid fruit.

On the other hand, grasping with a fixed pose is the easiest approach for robotic manipulation, which has been widely adopted in commercial fruit packaging robots, but it is prone to fail without feedback. Thus, grasp planning is the premise for robotic manipulation. Different from parallel-jaw or multi-finger to determine the contact points^[21,22], there is a larger contact surface for suction grasp^[23]. Point clouds are commonly used for robot manipulation planning^[24,25] and are appropriate for determining the contact surface. Both traditional methods^[25,26] and deep learning methods^[27-30] have been studied for grasp planning. However, few researchers have considered the suction mechanism and these methods are only suitable for objects with a flat surface^[31]. Hence, it is necessary to develop a suction scheme suitable for spheroid fruit packaging robots^[32].

This study aimed to explore the suction mechanism and develop a suction region selection algorithm. And furthermore, achieve the automated packaging of apples with less damage.

2 Materials and methods

2.1 Materials and system setup

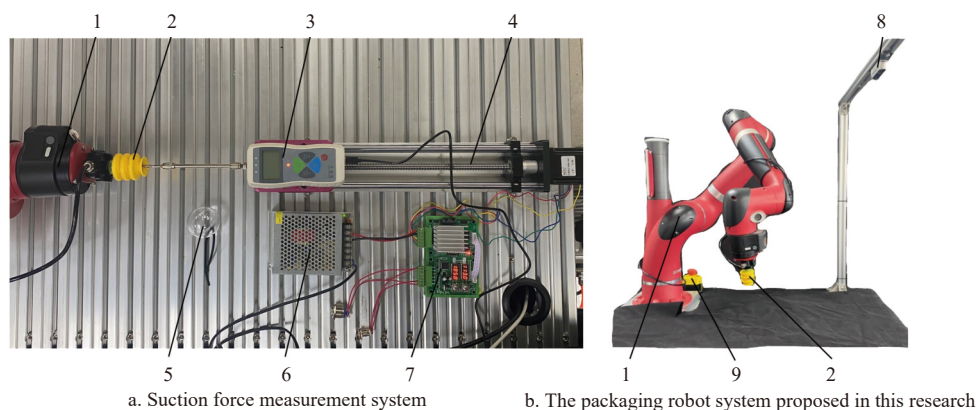
In this research, a total of 42 Fuji apples were used to carry out the experiment. The weights and the morphological indicators, such as heights, diameters and radiuses were measured in the first place. 3D printing technology was adopted to manufacture the suction

cups. The suction cups were fabricated by a 3D printer (Dreamer, Shanzhu, China) and thermoplastic elastomer (TPE, eSUN, China) printing material. The TPE printing material has been widely used for flexible 3D printing and has many advantages, such as high strength, good elasticity and wear resistance. The printed flexible suction cups could be applied in food, medical and other fields directly.

As shown in Figure 1, a suction force measurement system and a packaging robot system were set up for experiment. For the suction force measurement system in Figure 1a, the printed suction cup was attached at the end of the robot manipulator (Sawyer, Rethink, USA) with 7 degree-of-freedom and 4 kg maximum load. The suction cup was also controlled by an air pump through tubing. The dynamometer (Aidebao, China) was mounted on the electric sliding table, which was powered by a 24 VDC power supply and controlled by a stepper motor controller (YF-31, China). As for the packaging robot system in Figure 1b, the robot manipulator and the suction cup were installed in the same way as the suction force measurement system. In addition, a depth camera (RealSense D435i, Intel, USA)^[33,34] based on active stereo technology was mounted for object detection and optimal suction region selection. The processor of the robot control platform was an Intel Core i7-11700@2.5 GHz, with 16 GB RAM, 1.5 TB hard disk, and NVIDIA RTX 3060 GPU with 12 GB video memory. The suction region selection algorithm and the robot control system were developed and integrated by ROS Melodic based on Ubuntu 18.04 Linux operating system.

2.2 Methods

First, the suction cups were designed based on the geometric and morphological indicators of the apples. The suction contact mechanism was also analyzed in this section. Next, an optimal suction region selection algorithm was developed based on geometric information. On the basis of the above design and algorithm, a robotic apple packaging system was developed to realize pick-and-place demonstration.



1. Robot manipulator 2. Suction cup 3. Dynamometer 4. Electric sliding table 5. Acrylic ball 6. Power 7. Controller 8. Depth camera 9. Emergency button

Figure 1 System setup

2.2.1 Design of suction cups based on geometric indicators

There are two main requirements for robotic manipulation based on suction: 1) the ability to form a sealed region, which depends on the material and structure of suction cups; 2) the ability to provide a reliable suction force. Although there are various structures of the suction cups designed for commercial purposes, they are unsuitable for fruit manipulation. For this reason, on the basis of the morphological indicators and the suction contact mechanism, we designed a suction cup with a circular cross-section,

as shown in Figure 2a. The diameter of the suction port is defined as d_s . In order to provide reliable suction force for the spherical objects, a spherical curved surface is added outside the suction port. Similarly, the diameter of the curved surface is defined as D_s . The curvature radius of the spherical curved surface is defined as R_s . The three parameters (d_s , D_s , and R_s) mentioned above are illustrated in Figure 2b. Figure 2c shows the mechanism of the suction contact with different surface curvature diameters of objects. There are two situations during the suction process: when

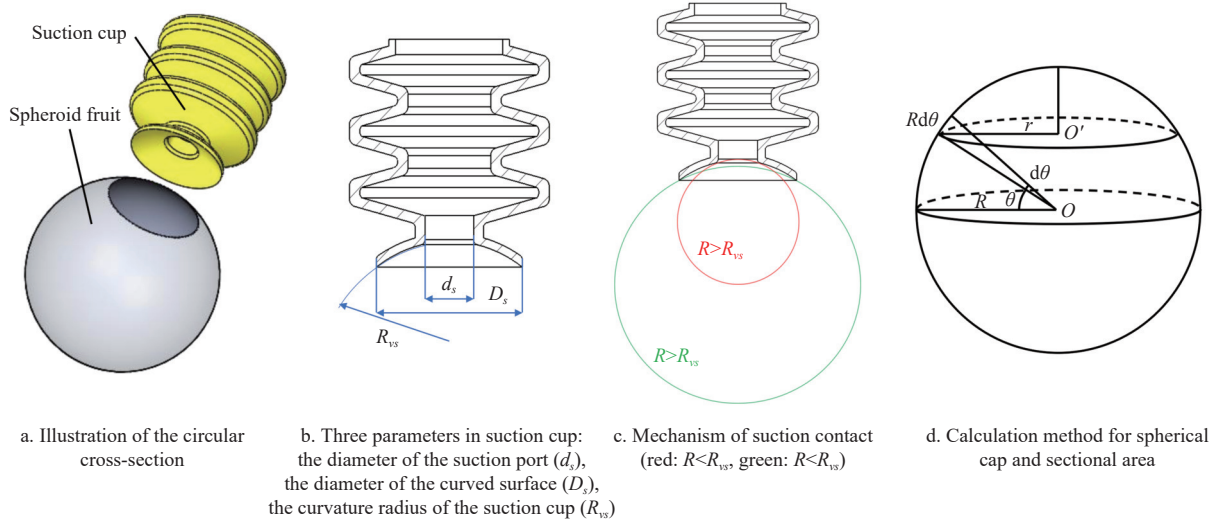


Figure 2 Design of the suction cup

the curvature radius of the suction area of the object is smaller than R_{vs} , the seal ring is formed between the suction port and object (represented as red in Figure 2c). On the contrary, the edge of the vacuum chuck will form a seal ring with the object's surface (represented as green in Figure 2c).

Next, the equation to calculate the suction force and the area of contact surface will be introduced. The suction force F is related to the contact area with the fruit, which can be calculated through Equation (1).

$$F = PA \quad (1)$$

where, P denotes the vacuum level inside the suction cup (due to the leakage of vacuum, the degree of vacuum is usually 0.04 or 0.06 MPa); A is the contact area between the suction cup and the object, m^2 . Specifically, whether it is cross-sectional area or spherical cap area will be further explored with experiment in Section 3. The sectional area S_{sa} can be calculated through Equation (2).

$$S_{sa} = \pi R^2 \cos^2 \theta \quad (2)$$

where, R denotes the radius of the objects, m ; θ is the angle ($^\circ$) between seal ring and equator from the center of sphere O , as shown in Figure 2d. θ can be calculated through Equation (3).

$$\theta = \begin{cases} \cos^{-1} \frac{d_s}{R}, & R < \frac{R_{vs}}{2} \\ \cos^{-1} \frac{D_s}{R}, & R \geq \frac{R_{vs}}{2} \end{cases} \quad (3)$$

where, d_s is the diameter of the suction port, and R_{vs} is the curvature

radius of the suction cup. Besides, different sizes of objects could lead to difference in spherical cap area though they are in the same situation illustrated in Figure 2c. Another contact area, the spherical cap area S_{sca} , can be calculated through Equation (4).

$$S_{sca} = \int_{\theta}^{\frac{\pi}{2}} 2\pi r R d\theta \quad (4)$$

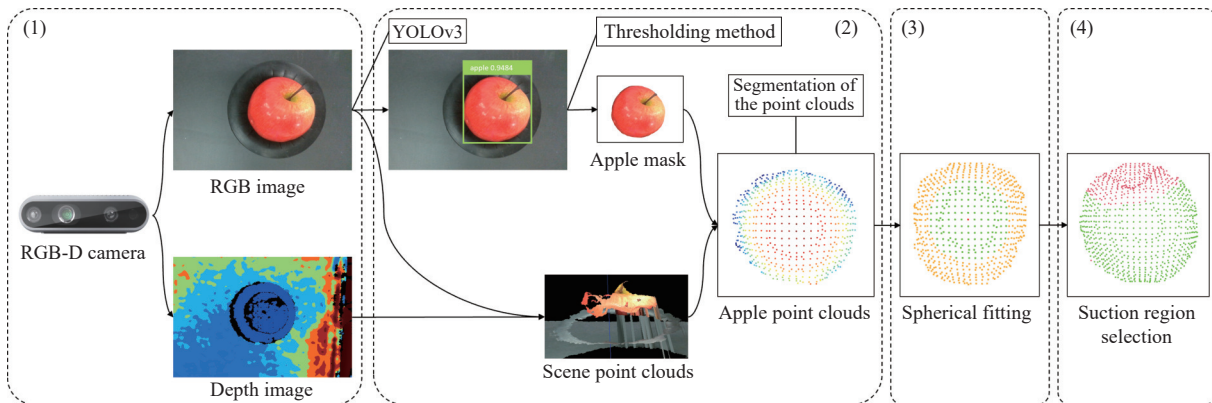
where, r denotes the radius of the seal ring, m . After solving the definite integral in Equation (4), the spherical cap area S_{sca} can be calculated as follows:

$$S_{sca} = 2\pi R^2 (1 - \sin \theta) \quad (5)$$

2.2.2 Optimal suction region selection algorithm based on geometric information

According to Equation (1), larger contact area can provide more reliable suction force. Obviously, the situation annotated as green color in Figure 2c could ensure a larger contact area between the suction cup and the objects. Thus, an algorithm based on geometric information is supposed to integrate into the robot system to avoid the situation annotated as red color. The proposed optimal suction region selection algorithm mainly involves four steps: (1) RGB-D information acquisition, (2) object detection and point cloud generation, (3) spherical fitting, and (4) suction region selection. The entire pipeline is illustrated in Figure 3.

First, RGB-D image pair of the scene is obtained from the RealSense depth camera. Before the optimal selection of the suction region, the scene point clouds need to be generated and segmented



Note: Mainly consists of four steps: (1) RGB-D information acquisition, (2) object detection and point cloud generation, (3) spherical fitting, and (4) suction region selection. In the final point clouds, the green points represent the regions recommended for suction. The red points represent the regions not recommended for suction.

Figure 3 The overall workflow of the optimal suction region selection algorithm based on geometric information

to remove the background. The color image is used to acquire the Region of Interest (ROI) by the YOLOv3 model, a real-time object detection network. In order to obtain the mask of the apple, a series of image processing pipelines are adopted on the ROI area, such as threshold segmentation, contours find, morphological manipulation, and binary image segmentation. Finally, the apple point clouds could be segmented from the scene point clouds using the apple mask and a plane. After that, spherical fitting is carried out to analyze the apple's surface for optimal suction region selection. Spherical fitting is performed on the point clouds depending on the parameters of the suction cup. Specifically, all points were saved within a set diameter around each point as a local point cloud and perform the spherical fitting. The results contain the center coordinate and the curvature radius of the set spherical area after spherical fitting. The spherical fitting is realized by solving the spherical equation, which is given by:

$$(x - x_0)^2 + (y - y_0)^2 + (z - z_0)^2 = R_{sf}^2 \quad (6)$$

where, (x, y, z) is the coordinates of each point in the point clouds, (x_0, y_0, z_0) is the center coordinate of the fitted sphere, and R_{sf} is the radius of the fitted sphere. The shape determination coefficient E represents the sum of squares of the distance from each point on the point cloud to the fitted spherical surface, which can be calculated from Equation (7).

$$E = \sum_{i=0}^n [(x - x_0)^2 + (y - y_0)^2 + (z - z_0)^2 - R_{sf}^2]^2 \quad (7)$$

The expected results are the x_0 , y_0 , z_0 , and R_{sf} that satisfy the minimum of E . The following linear equation is obtained by the method of seeking partial derivatives.

$$\begin{bmatrix} \bar{x}^2 - \bar{x}^2 & \bar{xy} - \bar{x}\bar{y} & \bar{xz} - \bar{x}\bar{z} \\ \bar{xy} - \bar{x}\bar{y} & \bar{y}^2 - \bar{y}^2 & \bar{yz} - \bar{y}\bar{z} \\ \bar{xz} - \bar{x}\bar{z} & \bar{yz} - \bar{y}\bar{z} & \bar{z}^2 - \bar{z}^2 \end{bmatrix} \begin{bmatrix} x_0 \\ y_0 \\ z_0 \end{bmatrix} = \begin{bmatrix} (\bar{x}^3 - \bar{x}\bar{x}^2) + (\bar{xy}^2 - \bar{x}\bar{y}^2) + (\bar{xz}^2 - \bar{x}\bar{z}^2) \\ (\bar{x}^2\bar{y} - \bar{x}^2\bar{y}) + (\bar{y}^3 + \bar{y}\bar{y}^2) + (\bar{yz}^2 - \bar{y}\bar{z}^2) \\ (\bar{x}^2\bar{z} - \bar{x}^2\bar{z}) + (\bar{zy}^2 - \bar{z}\bar{y}^2) + (\bar{z}^3 - \bar{z}\bar{z}^2) \end{bmatrix} \quad (8)$$

All the point clouds on the apple are traversed with the spherical fitting step to find their corresponding R_{sf} . Finally, according to the relationship between R_{sf} and R_{vs} , the apple point clouds could be divided into two categories: (1) point clouds with $R_{sf} < R_{vs}$, which has lower success rate for suction, (2) point clouds with $R_{sf} \geq R_{vs}$, which has higher success rate for suction. The grasp region selection result p can be expressed as:

$$p = \begin{cases} 0, & R_{sf} < R_{vs} \\ 1, & R_{sf} \geq R_{vs} \end{cases} \quad (9)$$

where, "0" indicates that the region is not recommended for robotic suction, while "1" refers to the region is recommended.

2.2.3 Robot system integration

Due to the static off-line packaging mode in this research, the relative position between the base link of the robotic arm and the objects was fixed. Thus, the Eye-to-Hand hand eye calibration mode was adopted in this system, rather than Eye-in-Hand mode. The depth camera was installed at a height of 800 mm above the platform, as shown in Figure 1b. In terms of software design, the RGB images and depth images collected by the camera was received by the robot system through a USB 3.0 port and was published in "topic" form. Then, the robot manipulator subscribed the published "topic" and performed the suction region selection

algorithm introduced in Section 2.2.2. Finally, the MoveIt! module in ROS was called by the robot manipulator to perform path planning and achieve the suction manipulation.

3 Experiments and results

In this section, the parameters of the suction cups were determined in the first place and the suction grasping mechanism was explored with our suction force measurement system. Furthermore, we carried out the experiments to evaluate the suction region selection algorithm and the robotic apple packaging system. In addition, early stage bruise of the experimental apples was detected by spatial-frequency domain imaging (SFDI) technology for validation.

3.1 Parameters determination for suction cups

In order to determine the parameters of the suction cups, the weight and the most important morphological indicators of the experimental apples were measured, including height and diameter. The spherical fitting method introduced in Section 2.2.2 was also used to evaluate the radius of the apple surface. The maximum and minimum values of these indicators are listed in Table 1. In the suction force measurement experiment, acrylic balls were also employed to explore the influence of the physical properties, such as surface roughness. The diameters of the acrylic balls were determined to be 30, 40, 50, 60, 70, 80, 90, and 100 mm, which covers all sizes of the experimental apples.

Table 1 Weight and morphological indicators of the apples used for experiment

	Weight/g	Height/mm	Diameter/mm	Radius/mm
Minimum	87.86	39.65	57.32	26.5
Maximum	319.90	93.62	94.48	47.5

As introduced in Section 2.2.1, the three parameters (d_s , D_s , and R_{vs}) of the suction cups need to be determined for further study. The situation annotated in red color in Figure 2c was considered to determine d_s . In order to provide sufficient suction force for the heaviest apple, the diameter of the suction port d_s is calculated to be 9.98 mm (when $P=0.04$ MPa) and 8.16 mm (when $P=0.06$ MPa) according to Equation (1). Therefore, the diameter of the suction port d_s was set to 10 mm to provide more reliable suction force. Besides, the diameter of the suction cup curved surface D_s was set to 30 mm. The curvature radius of the spherical curved surface (R_{vs}) is one of the most critical parameters in suction cups. The relationship between R_{vs} and the radius of the apple need to be explored in the following experiment, depending on the measurement results of the morphological indicators. Hence, three suction cups with various R_{vs} (25 mm, 30 mm, and 35 mm) were printed, which were smaller than, equal to and larger than the minimum radius of the experimental apples. The whole parameters of the three suction cups are listed in Table 2.

Table 2 Parameters of the printed suction cups for experiments

No.	d_s /mm	D_s /mm	R_{vs} /mm
1	10	30	25
2	10	30	30
3	10	30	35

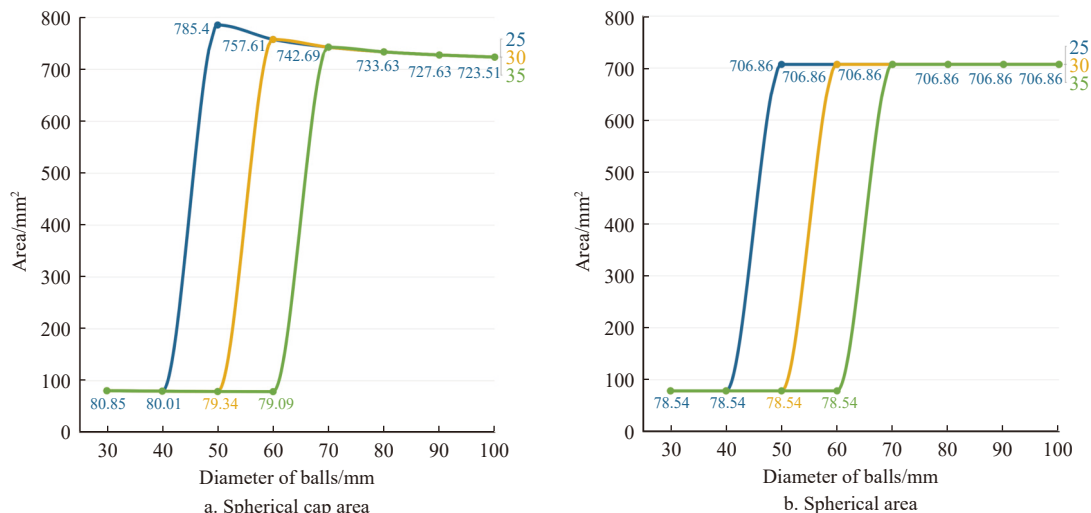
3.2 Results for contact area calculation

When different sizes of suction cups sucking different sizes of acrylic balls, the sectional area and the spherical cap area could be calculated theoretically through Equations (2) and (5), respectively.

The calculation results and the trends are shown in Figure 4, which will be used for further suction force analysis in the following experiments.

As can be seen from Figure 4, with the increasement of diameter of the acrylic balls, both the spherical cap area and the sectional area will have a substantial increasement. The reason for

this is the contact condition changed from the situation annotated in red color to green color illustrated in Figure 2c. In addition to this, under the same contact situation, the spherical cap area will slightly decrease with the increasement of diameter of acrylic balls. On the other hand, the sectional area remains unchanged, due to different suction cups have the same size in both d_s and D_s .



Note: 25, 30, 35 means the R_{vs} of the suction cups, mm.

Figure 4 Relationship between the contact area (both spherical cap area and sectional area) and the diameters of the acrylic balls

3.3 Results for suction force measurement

Based on the measurement system introduced in Figure 1a, some important factors in robotic suction grasping were taken into consideration and explored, including output pressure of the air pump, R_{vs} of the suction cups, sizes and physical properties of the objects. Three different sizes of suction cups introduced above were installed at the end of the robot manipulator for experiments. The

suction force was tested at five levels of the air pump output, from 0.1 to 0.5 MPa with 0.1 MPa step increment. The speed of the electric sliding table was set to 2 cm/min during the experiment. It is worth noting that, the suction cup was collinear with the object and the measuring head of the dynamometer. This was to eliminate the influence of weight and gravity of the suction objects. The results of the acrylic balls are shown in Figure 5.

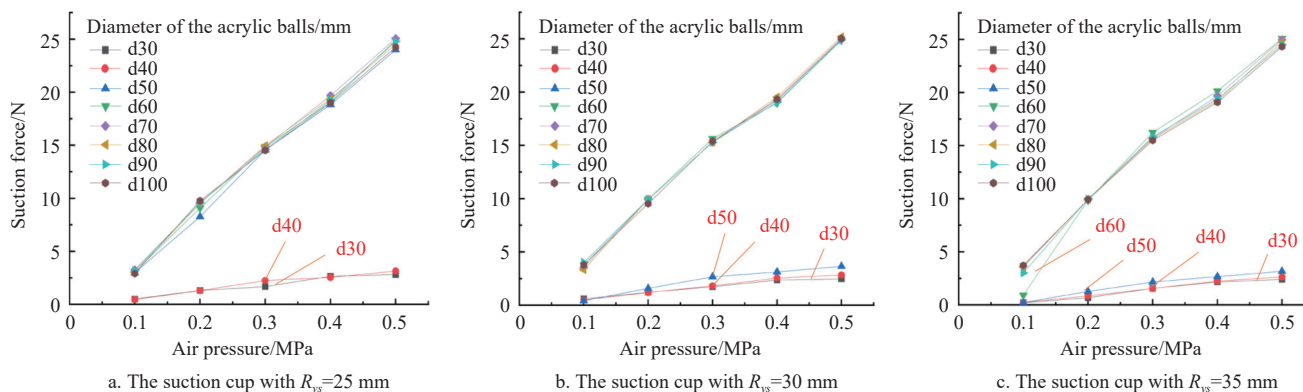


Figure 5 Results of suction force measurement for the acrylic balls

As can be seen, the suction force has a linear relationship with the air pressure. Thus, Equation (1) was verified. Besides, the suction force is similar among the three suction cups in the same situation, which demonstrated that they have the same contact region. From another point of view, under the same air pump output, the influence of the ball size on suction force is not significant. At a significance of 5%, the three sets of data can be considered approximately equal with p -value=0.98. In other words, the suction force did not decrease with the increasement of the size of the balls. In combination with the trends in Figure 4, we can draw the conclusion that, the suction force has a linear relationship with the sectional area, rather than spherical cap area. As can be seen

from the line chart, when the radius of the object is smaller than that of the suction cup, the contact region becomes the suction port, and the suction force is not enough for manipulation in this case. We can also draw another important conclusion that, the suction cup with smaller R_{vs} is more likely to provide enough suction forces, and the suction cup with $R_{vs} = 25$ mm was selected for robot system integration. Similar results could be observed in the suction force measurement of apples in Figure 6.

When the radius of the suction region on the apple surface is smaller than R_{vs} , the contact region is the suction port and the contact area is too small to provide suction force larger than 3.2 N for manipulation. In the opposite case, reliable suction forces could

be provided with the increment in air pump output. Besides, by comparing Figure 5 with Figure 6, in the same condition, there is little difference in suction force between the acrylic balls and the apples. At a significance of 5%, the data can be considered

approximately equal with p -value = 0.88. In Figure 7, the box plot of the suction force for both acrylic balls and apples were provided. In addition, linear fitting with least square method between the suction force and the air pressure was also performed.

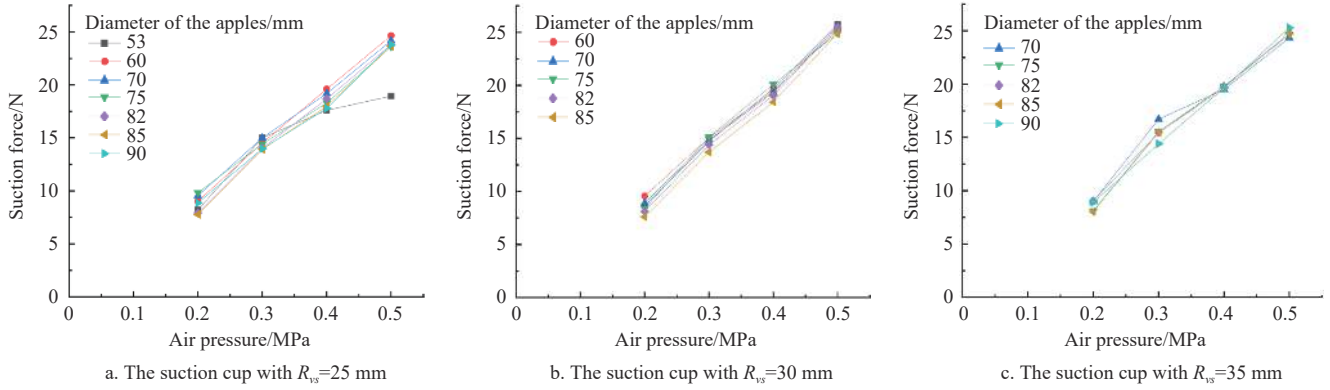


Figure 6 Results of suction force measurement for the apples

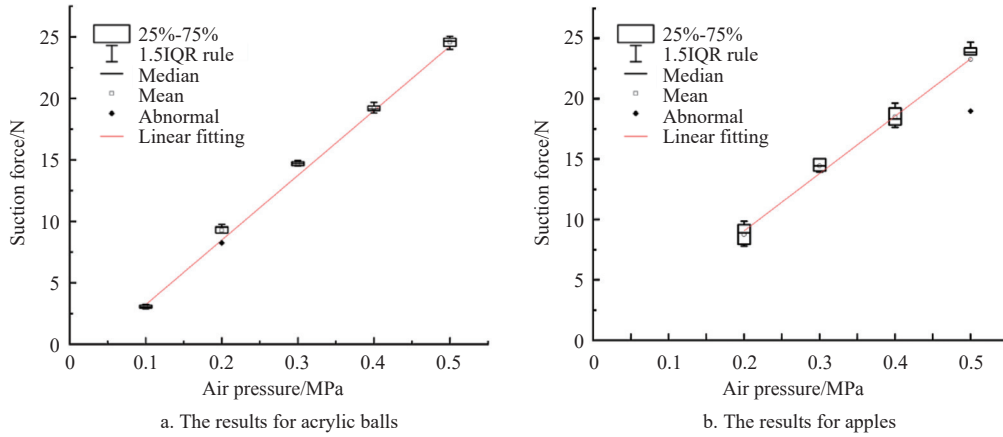


Figure 7 Linear fitting of the relationship between the suction force and the air pressure

The fitted suction force of the acrylic balls was:

$$F_{(\text{ball})} = \begin{cases} 0, & p < 0.0032 \text{ MPa} \\ 52.93p - 1.7, & p \geq 0.0032 \text{ MPa} \end{cases}$$

where, p is the output pressure of the air pump. Similarly, the suction force of the apples is given by:

$$F_{(\text{apple})} = \begin{cases} 0, & P < 0.018 \text{ MPa} \\ 49.52P - 0.9, & P \geq 0.018 \text{ MPa} \end{cases}$$

Considering the apples' gravity, the starting air pressure was set to 0.018 MPa to provide suction force more than 3.2 N. The correlation coefficients R^2 for acrylic balls and apples were 0.9949 and 0.9837, respectively. Comparing these two results on linear fitting, the conclusion can be validated that the physical property (such as surface roughness) of apples did not cause a significant influence on the final suction force. In summary, we choose the suction cup with $R_{vs} = 25$ mm to ensure reliable suction force could be provided.

3.4 Results for suction region selection

In order to validate the suction region selection algorithm introduced in Section 2.2.2, experiments were performed on apples with different orientation and pose. Figure 8 is the results for suction region selection and suction grasping condition.

The suction region selection algorithm takes RGB image and depth image as input. And output the recommended regions for robotic suction grasping. As can shown in Figure 8, most of the

point clouds annotated in red color located at the stem and calyx parts of the apple, where the radius of the curvature is smaller than 25 mm. This indicates that the suction cup cannot provide reliable suction force on these regions. On the other hand, most of the point clouds annotated in green color located at the side surface of the apple, where the radius of the curvature is larger than 25 mm and meets the basic requirements of a successful suction grasping.

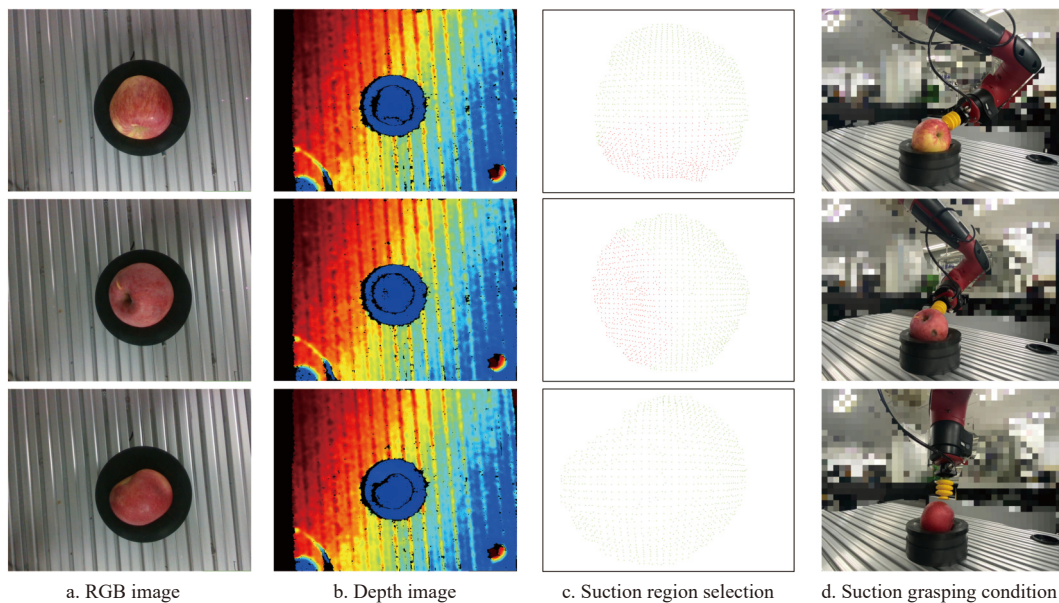
3.5 Results for success rate of suction grasping

In this experiment, the experimental apples were divided into three groups (small, medium, and large), according to the diameter. The pick-and-place action was conducted for 30 times for each group. The results for success rate of suction grasping are listed in Table 3.

Table 3 Success rate of suction grasping for apples in different sizes

Size	Total number	Failed	Dropped	Success	Success rate/%
Small (≤ 70 mm)	30	4	0	26	86.67
Medium (> 70 mm and ≤ 80 mm)	30	2	3	25	83.33
Large (> 80 mm)	30	1	4	25	83.33

The average success rate for suction grasping was 84.44%. During the experiment, a total of 14 attempts failed. Among them, 7 suction grasping attempts failed in the early stage to pick up the apples. The main reason was that the error in positioning, calibration and suction region selection. Apples with smaller size



Note: In Figure 8c, the green points represent the regions recommended for suction. The red points represent the regions not recommended for suction.

Figure 8 Results for suction region selection algorithm and suction grasping condition

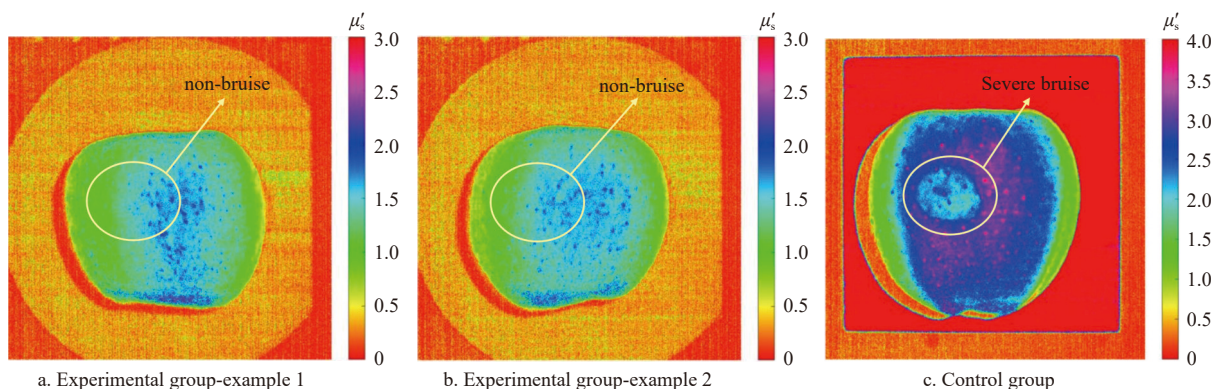
tend more to get into trouble in this stage. Another 7 suction attempts picked the apples successfully, but failed by dropping or slipping. Apples with larger size tend more to get into trouble in this stage. The main reason was that the acceleration of the robot manipulator and the weight of the apples. For better illustration, we also provide the demonstration video of our robotic apple packaging system in the following YouTube channel: https://youtu.be/RJ5EkA_Si1s.

3.6 Early stage bruise detection and validation

Early stage bruise is quite common for fragile fruit after robotic manipulation, which is difficult to be detected by visible light and machine vision. This could also affect the added value of the fruit. In addition, SFDI technology was adopted in this experiment for further validation. The method was developed and explained in

detail in our previous work^[35-37], which could detect the early stage bruise in apples. In the experiment, the apples in experimental group were used to perform pick-and-place action by the packaging robot system in this study. The apples in control group were impacted by external force. We obtained the SFDI images at 730 nm wavelength and 0 , $\frac{2}{3}\pi$ and $\frac{4}{3}\pi$ phase position within 2 h. Diffusion images were obtained through image calibration and image demodulation steps. Reduced scattering coefficient mappings (μ'_s) were finally obtained through curve fitting step and were shown in Figure 9.

The comparison results demonstrated that the developed packaging robot system did not cause additional damage or early stage bruise to the apples in experimental group.



Note: The regions for comparison of the early stage bruise were all annotated in the figure.

Figure 9 Reduced scattering coefficient mappings (μ'_s) of the apples in experimental group (manipulated by packaging robot in this study) and control group (impacted by external force)

4 Discussion

On the basis of the issues in this study, further studies are supposed to carry out. First of all, major attention was paid on the curvature radius of the suction cups. Other parameters could be further explored, such as the diameter of the suction port and the diameter of the curved surface. Materials adopted to print the suction cup and fatigue time of the materials also deserve

exploration. Thus, a more comprehensive and scientific guidance could be provided to suction cup design and manufacturing. Secondly, there are two different suction actions: picking and cutting. Picking means that the suction force is in the same or opposite direction with gravity, while cutting means that the suction force is not co-linear with gravity (usually vertical). In this research, we adopted cutting mode to eliminate the influence of gravity on the suction force measurement results. However, picking mode is the

major action during fruit packaging and manipulation. Therefore, further studies can focus on the picking mode. In the third place, the suction region selection algorithm developed in this research adopted point cloud in the single view. Multi-view 3D reconstruction algorithms could be performed before the suction region selection process to achieve completed and optimized selection of suction region. In addition, on the basis of deep learning, end-to-end suction region selection methods appropriate for spheroid fruit are supposed to study in the future.

5 Conclusions

In this research, on the basis of the geometric features, a reliable and robust structure of suction cup was designed for robotic apple packaging. Three suction cups with different curvature radius (25, 30, 35 mm) were manufactured for experiment. The results on suction force measurement of acrylic balls and apples demonstrated that, there is a linear relationship between the air pressure and the suction force. The correlation coefficients R^2 for acrylic balls and apples were 0.9949 and 0.9837, respectively. The physical property of apples did not cause significant influence on the suction force, such as surface roughness. The conclusion indicates us to design and choose the suction cups with smaller curvature radius than spheroid objects. On the basis of the geometric information, the optimized selection of suction regions strategy was developed and integrated into the robotic apple packaging system. The goal of suction grasping of apples was achieved, with 84.44% success rate on average in 90 attempts. Finally, the method based on SFDI technology was adopted for early stage bruise detection and validation. The above results and conclusions indicate that the suction based robotic system can provide guidance for automated apple packaging.

Acknowledgements

This research was supported and funded by the National Natural Science Foundation of China under Grant No. U20A2019. The authors appreciate the funding organisation for their financial supports. The authors would also like to thank the helpful comments and suggestions provided by editor and the anonymous reviewers.

[References]

- [1] Zhang Z, Lu Y Z, Lu R F. Development and evaluation of an apple infield grading and sorting system. *Postharvest Biology and Technology*, 2021; 180: 111588.
- [2] Zhao M, Peng Y K, Li L. A robot system for the autodetection and classification of apple internal quality attributes. *Postharvest Biology and Technology*, 2021; 180: 111615.
- [3] Wang Z H, Xun Y, Wang Y K, Yang Q H. Review of smart robots for fruit and vegetable picking in agriculture. *Int J Agric & Biol Eng*, 2022; 15(1): 33–54.
- [4] Zeng A, Yu K-T, Song S R, Suo D, Walker E, Rodriguez A, et al. Multi-view self-supervised deep learning for 6d pose estimation in the amazon picking challenge. 2017 IEEE International Conference on Robotics and Automation (ICRA), IEEE, 2017. doi: [10.1109/ICRA.2017.7989165](https://doi.org/10.1109/ICRA.2017.7989165)
- [5] Corbato C H, Bharatheesha M, Van Egmond J, Ju J H, Wisse M. Integrating different levels of automation: Lessons from winning the amazon robotics challenge 2016. *IEEE Transactions on Industrial Informatics*, 2018; 14(11): 4916–4926.
- [6] Zeng A, Song S R, Yu K-T, Donlon E, Hogan F R, Bauza M, et al. Robotic pick-and-place of novel objects in clutter with multi-affordance grasping and cross-domain image matching. *The International Journal of Robotics Research*, 2019; 41(7): 690–705.
- [7] Aoyagi S, Suzuki M, Morita T, Takahashi T, Takise H. Bellows suction cup equipped with force sensing ability by direct coating thin-film resistor for vacuum type robotic hand. *IEEE/ASME Transactions on Mechatronics*, 2020; 25(5): 2501–2512.
- [8] Zhang B H, Xie Y X, Zhou J, Wang K, Zhang Z. State-of-the-art robotic grippers, grasping and control strategies, as well as their applications in agricultural robots: A review. *Computers and Electronics in Agriculture*, 2020; 177: 105694.
- [9] Wang L-J, Zhang Q, Song H Y, Wang Z-W. Mechanical damage of ‘Huangguan’ pear using different packaging under random vibration. *Postharvest Biology and Technology*, 2022; 187: 111847.
- [10] Eppner C, Höfer S, Jonschkowski R, Martin-Martín R, Sieverling A, Wall V, et al. Four aspects of building robotic systems: lessons from the Amazon Picking Challenge 2015. *Autonomous Robots*, 2018; 42(7): 1459–1475.
- [11] Hasegawa S, Wada K, Niitani Y, Okada K, Inaba M. A three-fingered hand with a suction gripping system for picking various objects in cluttered narrow space. 2017 IEEE/RSJ International Conference on Intelligent Robots and Systems (IROS), IEEE, 2017. doi: [10.1109/IROS.2017.8202288](https://doi.org/10.1109/IROS.2017.8202288)
- [12] Zhang B H, Zhou J, Meng Y M, Zhang N, Gu B X, Yan Z H, Idris S I. Comparative study of mechanical damage caused by a two-finger tomato gripper with different robotic grasping patterns for harvesting robots. *Biosystems Engineering*, 2018; 171: 245–257.
- [13] Liu C-H, Huang G-F, Chiu C-H, Pai T-Y. Topology synthesis and optimal design of an adaptive compliant gripper to maximize output displacement. *Journal of Intelligent & Robotic Systems*, 2018; 90(3): 287–304.
- [14] Hughes J, Scimeca L, Ifrim I, Maiolino P, Iida F. Achieving robotically peeled lettuce. *IEEE Robotics and Automation Letters*, 2018; 3(4): 4337–4342.
- [15] Kurpaska S, Sobol Z, Pedryc N, Hebda T, Nawara P. Analysis of the pneumatic system parameters of the suction cup integrated with the head for harvesting strawberry fruit. *Sensors*, 2020; 20(16): 4389.
- [16] Zhakypov Z, Heremans F, Billard A, Paik J. An origami-inspired reconfigurable suction gripper for picking objects with variable shape and size. *IEEE Robotics Automation Letters*, 2018; 3(4): 2894–2901.
- [17] Gilday K, Lilley J, Iida F. Suction cup based on particle jamming and its performance comparison in various fruit handling tasks. 2020 IEEE/ASME International Conference on Advanced Intelligent Mechatronics (AIM), IEEE, 2020. doi: [10.1109/AIM43001.2020.9158945](https://doi.org/10.1109/AIM43001.2020.9158945).
- [18] Uppalapati N K, Walt B, Havens A J, Mahdian A, Chowdhary G, Krishnan G. A berry picking robot with a hybrid soft-rigid arm: design and task space control. *Robotics: Science and Systems*, 2020. doi: [10.15607/RSS.2020.XVI.027](https://doi.org/10.15607/RSS.2020.XVI.027).
- [19] Koivikko A, Drotlef D-M, Dayan C B, Sariola V, Sitti M. 3D-printed pneumatically controlled soft suction cups for gripping fragile, small, and rough objects. *Advanced Intelligent Systems*, 2021; 3(9): 2100034.
- [20] Aoyagi S, Morita T, Shintani T, Takise H, Takahashi T, Suzuki M. Formation of PVDF piezoelectric film on 3D bellows surface of robotic suction cup for providing force sensing ability-feasibility study on two methods of dip-coating and lamination. 2019 IEEE/RSJ International Conference on Intelligent Robots and Systems (IROS), IEEE, 2019. doi: [10.1109/iros40897.2019.8967654](https://doi.org/10.1109/iros40897.2019.8967654).
- [21] Seo J, Kim S, Kumar V. Planar, bimanual, whole-arm grasping. 2012 IEEE International Conference on Robotics and Automation, IEEE, 2012.
- [22] Zhao Z ZH, Shang W W, He H Y, Li Z J. Grasp prediction and evaluation of multi-fingered dexterous hands using deep learning. *Robotics and Autonomous Systems*, 2020; 129: 103550.
- [23] Giefer L A, Arango Castellanos J D, Babr M M, Freitag M. Deep learning-based pose estimation of apples for inspection in logistic centers using single-perspective imaging. *Processes*, 2019; 7(7): 424.
- [24] Mahler J, Pokorny F T, Hou B, Roderick M, Laskey M, Aubry M, et al. Goldberg. Dex-net 1.0: A cloud-based network of 3d objects for robust grasp planning using a multi-armed bandit model with correlated rewards. 2016 IEEE International Conference on Robotics and Automation (ICRA), IEEE, 2016.
- [25] Valencia A J, Idrovo R M, Sapp A D, Guingla D P, Ochoa D. A 3D vision based approach for optimal grasp of vacuum grippers. 2017 IEEE International Workshop of Electronics, Control, Measurement, Signals and Their Application to Mechatronics (ECMSM), IEEE, 2017.
- [26] Gori I, Pattacini U, Tikhonoff V, Metta G. Three-finger precision grasp on incomplete 3d point clouds. 2014 IEEE International Conference on Robotics and Automation (ICRA), IEEE, 2014.
- [27] Mahler J, Liang J, Niyaz S, Laskey M, Doan R, Liu X Y, et al. Dex-net 2.0: Deep learning to plan robust grasps with synthetic point clouds and analytic grasp metrics. arXiv preprint, 2017.

- [28] Park K, Prankl J, Vincze M. Mutual hypothesis verification for 6D pose estimation of natural objects. Proceedings of the IEEE International Conference on Computer Vision Workshops, 2017.
- [29] Mahler J, Matl M, Liu X Y, Li A, Gealy D, Goldberg K. Dex-net 3.0: Computing robust vacuum suction grasp targets in point clouds using a new analytic model and deep learning. 2018 IEEE International Conference on Robotics and Automation (ICRA), IEEE, 2018.
- [30] Utomo T W, Cahyadi A I, Ardiyanto I. Suction-based grasp point estimation in cluttered environment for robotic manipulator using deep learning-based affordance map. *International Journal of Automation and Computing*, 2021; 18(2): 277–287.
- [31] You F, Mende M, Štogl D, Hein B, Kröger T. Model-free grasp planning for configurable vacuum grippers. 2018 IEEE/RSJ International Conference on Intelligent Robots and Systems (IROS), IEEE, 2018.
- [32] Guo N, Zhang B H, Zhou J, Zhan K T, Lai S. Pose estimation and adaptable grasp configuration with point cloud registration and geometry understanding for fruit grasp planning. *Computers and Electronics in Agriculture*, 2020; 179: 105818.
- [33] Keselman L, Iselin Woodfill J, Grunnet-Jepsen A, Bhowmik A. Intel realsense stereoscopic depth cameras. Proceedings of the IEEE Conference on Computer Vision and Pattern Recognition Workshops, 2017.
- [34] Wang Q Y, Wu D H, Liu W, Lou M ZH, Jiang H Y, Ying Y B, Zhou M C. PlantStereo: A High Quality Stereo Matching Dataset for Plant Reconstruction. *Agriculture*, 2023; 13(2): 330.
- [35] Sun Z Z, Hu D, Xie L J, Ying Y B. Detection of early stage bruise in apples using optical property mapping. *Computers and Electronics in Agriculture*, 2022; 194: 106725.
- [36] Wang Q Y, Wu D H, Sun Z ZH, et al. Design, integration, and evaluation of a robotic peach packaging system based on deep learning. *Computers and Electronics in Agriculture*, 2023; 211: 108013.
- [37] Wang Q Y, Xing H, Ying Y B, Zhou M C. CGFNet: 3D Convolution Guided and Multi-scale Volume Fusion Network for fast and robust stereo matching. *Pattern Recognition Letters*, 2023; 173: 38–44.